Oncology Research, Vol. 24, pp. 463–475
Printed in the USA.

0965-0407/16 $90.00 + .00
DOI: http://dx.doi.org/10.3727/096504016X14685034103671
E-ISSN 1555-3906
www.cognizantcommunication.com

Inhibition of Proliferation, Migration, and Invasion by Knockdown of Pyruvate Kinase-M2 (PKM2) in Ovarian Cancer SKOV3 and OVCAR3 Cells

Yi Miao,[1] Meng Lu,[1] Qin Yan, Shuangdi Li, and Youji Feng

Department of Obstetrics and Gynecology, Shanghai General Hospital of Nanjing Medical University, Shanghai, P.R. China

Pyruvate kinase (PK) is a key enzyme in the process of glycolysis, catalyzing phosphoenolpyruvate (PEP) into pyruvate. Currently, PK isozyme type M2 (PKM2), one subtype of PK, has been proposed as a new tumor marker with high expression in various tumor tissues. Here we aimed to explore the effects of siRNA-PKM2 on ovarian carcinoma (OC) cell lines SKOV3 and OVCAR3, in which PKM2 was notably expressed. PKM2 gene interference lentivirus vectors were built by miRNA transfection assay. siRNA-PKM2-transfected SKOV3 and OVCAR3 cells were evaluated for cell proliferation, cell cycle distribution, cell apoptosis, cell migration, and invasion in this study. In addition, the expression levels of several tumor-related genes were measured using real-time PCR and Western blot. Results showed that siRNA-PKM2 markedly inhibited cell proliferation, induced apoptosis, and caused cell cycle arrest at the G_0/G_1 phase. Cell migration and invasion were significantly suppressed by siRNA-PKM2. Furthermore, the tumor-related genes caspase 7, Bad, and E-cadherin were upregulated, while MMP2, HIF1α, VEGF, and MMP9 were depressed by siRNA-PKM2. The function of siRNA-PKM2 on the biological behavior of OC cells indicated that PKM2 may also be a target for treatment of OC.

Key words: Pyruvate kinase isozyme type M2 (PKM2); Ovarian carcinoma (OC); Cell proliferation; Metastasis; Signaling pathway

INTRODUCTION

Ovarian cancer (OC) is one of the most common gynecological malignancies, with its incidence ranking third and mortality rate ranking first, and is a serious threat to the life of females (1). In recent years, with the improvement of surgery, new chemotherapy drugs and chemotherapy combined with traditional surgery and radiation therapy have been used for the treatment of OC. However, its recurrence rate in patients is still high, reaching about 40% to 60%, with the 5-year survival rate still hovering at 20% (2). In this context, biological therapy is receiving increased attention, including gene therapy (3).

Pyruvate kinase isozyme type M2 (PKM2) is one subtype of pyruvate kinase (PK), which is a key enzyme involved in the glycolysis progress. It was reported that PKM2 was expressed in various tissues, such as lung, adipose, pancreas islet, and all cells synthesizing a large number of nucleic acids, especially tumor cells (4). PKM2 will disappear in the process of tissue differentiation and will be expressed again in cancerization tissue (5). In addition, PKM2 is highly expressed in various tumor tissues, such as lung cancer, cervical cancer, and colon cancer; thus, it is evaluated as a new tumor marker and an important target in the development of cancer medication (6–8). Recently, it has been found that the expression levels of PKM2 were closely associated with a number of factors in tumors, including the malignant degree of tumors, angiogenesis, invasion and metastasis, drug resistance, and prognosis (9–11). Peng et al. proved that knocking down PKM2 in pancreatic cancer cells in vitro could significantly inhibit cell proliferation and induce cell apoptosis. Furthermore, in vivo, the tumor formation rates were decreased (12). Currently, the relationship between PKM2 and gynecologic cancer has also shown cause for concern. As early as 1978, it was reported that PKM2 was highly expressed in tissues of cervical cancer and endometrial cancer (13). Further, Kaura et al. found that the sensitivity and specificity of PKM2 in cervical cancer tissues between benign and malignant were 82% and 60%, respectively. Thus, PKM2 was regarded as a tumor marker in the cervical cancer screening process (14). Despite multiple evidence about the role of PKM2 in various cancers, the function of PKM2 remains largely unknown.

[1]These authors provided equal contribution to this work.
Address correspondence to Dr. Youji Feng, Department of Obstetrics and Gynecology, Shanghai General Hospital of Nanjing Medical University, No. 100 Haining Road, Hongkou District, 200080 Shanghai, P.R. China. E-mail: liaoyi1520@sina.com

In the current study, we measured the expression levels of PKM2 in OC and normal tissues in which the high expression of PKM2 in OC tissues was defined. After cell line screening, SKOV3 and OVCAR3 were determined to be our study targets. For both of the cell lines, knocking down PKM2 inhibited cell proliferation, caused cell cycle arrest at the G_0/G_1 phrase, induced cell apoptosis, and suppressed the capacity of cell migration and invasion. Moreover, the expression levels of several tumor-related genes were changed under the function of PKM2. The function of siRNA-PKM2 on the biological behavior of OC cells indicated that PKM2 may also be a target for OC treatment.

MATERIALS AND METHODS

Tissue Simples

To compare the mRNA expression levels of PKM2 in OC tissues and adjacent normal tissues, quantitative real-time polymerase chain reaction (qRT-PCR) was performed. Tissues were resected from 40 OC patients who were admitted to Shanghai General Hospital of Nanjing Medical University when the patients were undergoing definitive surgery, with peritumoral tissues within at least 5 cm of the tumor margin. According to the ethics committee guidelines, informed and written consent was obtained from all patients or their advisers. Ethical approval for the study was provided by the independent ethics committee of Shanghai General Hospital of Nanjing Medical University.

Immunohistochemistry Assay

Immunohistochemistry assay was performed to measure the protein levels of PKM2 in OC tissue and adjacent normal tissue. Briefly, the formalin-fixed and paraffin-wax-embedded (FFPE) 5-μm tissue sections were dewaxed and rehydrated. To unmask the antigen and inactivate endogenous peroxidase, the rehydrated sections were treated with 0.01 M of citrate buffer (pH 6). Sections were then heated twice in a microwave oven for 15 min, washed three times with 0.01 M of PBS, incubated with 5% (w/v) bovine serum albumin (BSA) at 37°C for 30 min, and subsequently at 4°C overnight with antibody: PKM2 (1:50; dissolved by 0.01 M of PBS; Abcam). The tissues were rinsed thoroughly in PBS three times, each time for 5 min, and incubated with a secondary antibody for 1 h at room temperature. The degree of steatosis and inflammation were analyzed under light microscope (magnification: 400×).

Cell Culture

Five human cell lines containing OC (C200, Caov3, SKOV3, HO8910, and OVCAR3) were obtained from Shanghai Cell Bank, Chinese Academy of Science (Shanghai, China). All cells were cultured in Dulbecco's modified Eagle's medium (DMEM; Hyclone, USA), supplemented with 100 μg/ml streptomycin, 10% heat-inactivated FBS, and 100 U/ml penicillin. All media were incubated in an incubator (Thermo Fisher Scientific Inc., Waltham, MA, USA) (37°C, 100% humidity, and 5% CO_2).

Small Interfering RNA Transfection

SKOV3 and OVCAR3 cells, which were selected to carry out our further experiments, were collected in the logarithmic growth phase, digested by trypsin, counted, and added to a six-well culture plate with 1 ml/well containing 5×10^5 cells/ml. Cells were then seeded in an antibiotic-free medium the day before transfection. After that, cells were transfected with 400 nmol/L of siRNA-PKM2™ or siRNA (as a negative control) using Lipofectamine 2000 (Invitrogen, Shanghai, China) according to the manufacturer's instructions. For siRNA-PKM2, RNA oligomers were synthesized in sense and antisense directions corresponding to human PKM2, containing three sections of the sequence: at nucleotides 871–893 (5′-GAGGTATTCCGATGCTTATTT-3′), 21 nucleotides; at nucleotides 1,335–1,357 (5′-TGGTGTTTGCGTCATT CAT-3′), 19 nucleotides; and at nucleotides 1,792–1,814 (5′-CCGCAAGCTGTTTGAAGAA-3′), 19 nucleotides. After 24, 48, and 72 h, cells were collected with each of the times regarded as one treated group and 0 h as a control for proliferation assay. The transfected cells at 48 h were used for the following cell adhesion assay, Transwell assay, qRT-PCR, and Western blot assay.

Cell Growth and Proliferation Assay

Cell Counting Kit-8 (CCK-8) Kit (Tongren, Shanghai, China) was used to assess the effects of siRNA-PKM2 on the viability of SKOV3 and OVCAR3 cells in different groups (control, negative control, and siRNA-PKM2 treatment groups). Briefly, CCK-8 reagent was added to each treated group of wells with 1:10 (v/v) per 100 μl of medium when cells were transfected for 0, 12, 48, and 72 h. After the endpoint of incubation, optical density (OD) at 450 nm was determined for the supernatant of each well by a microplate reader. Experiments were performed at least three times, each time in triplicate.

Flow Cytometry (FCM) Detection

Cell cycles were measured using propidium iodide (PI) and flow cytometry. In the treatment group, three groups of cells were incubated in cell culture solutions for 60 min and were seeded in six-well plates at a density of 3×10^5 cells/well. After being incubated for 48 h, cells were washed with PBS, trypsinized, and centrifuged at $1{,}000\times g$, 4°C, for 5 min. The obtained pellets were suspended with 300 μl of PBS containing 10% FBS and fixed in 700 μl of cold ethanol at −20°C for 24 h.

Then cells were washed twice with PBS and incubated in PBS containing RNaseA (1 mg/ml) for 10 min at 37°C. The samples were stained with PI (1 mg/ml) for 10 min, shielded from light, at room temperature. Finally, the cells were analyzed by flow cytometry (FACSCalibur; BD Biosciences, Franklin Lakes, NJ, USA), and the data were analyzed using CellQuest software (BD Biosciences).

On the other hand, apoptotic cells in the three groups were identified by flow cytometry and the Annexin-V/Fluorescein Isothiocyanate (FITC) kit (BD Biosciences). Briefly, SKOV3 and OVCAR3 cells were collected, resuspended in 200 µl of binding buffer containing 5 µl of Annexin-V/FITC, stained at 20°C–25°C in the dark for 10 min, centrifuged at room temperature (1,000×*g* for 5 min), resuspended in 200 µl of binding buffer again, then 10 µl of PI was added, mixed gently, and stained in an ice bath in the absence of light. After the above assays, flow cytometric analyses were performed.

Cell Migration Assay

SKOV3 and OVCAR3 cells in different groups (control, negative control, and siRNA-PKM2 treatment groups) were starved with serum-free RPMI-1640 medium (Hyclone) for 24 h before the following assays. Cells were digested for 5 min by 0.25% trypsin (Gibco, Shanghai, China) and resuspended in RPMI-1640 medium (Hyclone) containing 0.1% BSA. After counting, cells were diluted to 5×10^5 cells/ml, seeded in a 24-plate Transwell room, and then were continued to be incubated for 24, 48, and 72 h. Then cells were fixed for 15 min using 1 ml/well 4% paraformaldehyde (JRDUN Biotech, Shanghai, China), stained by Giemsa (JRDUN) for 30 min, and washed three times by 1× PBS. Finally, the Transwell room without migrating cells was wiped carefully using a cotton swab, placed under a 200× microscope, and the number of cells counted in random fields of 5–10.

Cell Invasion Assay

For cell invasion, before assays were performed, the Transwell room with an 8-µm pore size (Sigma-Aldrich, San Francisco, CA, USA) and 24 wells were washed with 1× PBS for 5 min. The inserts were coated with 80 µl of Matrigel (dilution at 1:2; BD Biosciences). Cells in 0.5 ml of serum-free medium with a density of 1×10^5 cells/ml were transferred to the upper Matrigel chambers. Then 0.75 ml of complete medium containing 10% FBS as chemoattractant was added to the lower chamber. Afterward they were incubated at 37°C for 48 h. Cells that were able to pass through the filter were fixed and stained by 1 ml of 0.5% crystal violet for 30 min. Finally, the numbers of invaded cells in five randomly selected high-power fields were counted under the microscope.

Quantitative Real-Time PCR (qRT-PCR) Assay

The mRNA levels of PKM2 in SKOV3 and OVCAR3 cells were quantified by qRT-PCR. Total RNA samples were isolated using TRIzol reagent (Invitrogen, Japan), and then the obtained mRNA was detected by agarose gel electrophoresis. cDNA was synthesized from approximately 5 µg of RNA using AMV reverse transcriptase

Table 1. Primers Used in qRT-PCR Analysis

Gene	Primer Sequence	Species	Amplicon Size (bp)
PKM2	Forward: 5′-TCTCCAGGGCACACCGTATTC-3′ Reverse: 5′-GCTGCTGAGGTCCTTTGGTTC-3′	Human	128
Caspase 7	Forward: 5′-ACCTATCCTGCCCTCACATC-3′ Reverse: 5′-TCTTCTCCTGCCTCACTGTC-3′	Human	108
MMP2	Forward: 5′-TTGACGGTAAGGACGGACTC-3′ Reverse: 5′-GGCGTTCCCATACTTCACAC-3′	Human	134
HIF1α	Forward: 5′-TCGGCGAAGTAAAGAATC-3′ Reverse: 5′-TTCCTCACACGCAAATAG-3′	Human	129
Bad	Forward: 5′-AGACCCGGCAGACAGATGAG-3′ Reverse: 5′-CTCTGGGCTGTGAGGACAAG-3′	Human	155
VEGF	Forward: 5′-ATTTCTGGGATTCCTGTAG-3′ Reverse: 5′-CAGTGAAGACACCAATAAC-3′	Human	157
MMP9	Forward: 5′-AAGGGCGTCGTGGTTCCAACTC-3′ Reverse: 5′-AGCATTGCCGTCCTGGGTGTAG-3′	Human	210
E-cadherin	Forward: 5′-GAGAACGCATTGCCACATACAC-3′ Reverse: 5′-AAGAGCACCTTCCATGACAGAC-3′	Human	164
GAPDH	Forward: 5′-CACCCACTCCTCCACCTTTG-3′ Reverse: 5′-CCACCACCCTGTTGCTGTAG-3′	Human	110

(Fermentas, USA). qRT-PCR reactions in a 25 µl total volume were performed using SYBR® Green 10× Supermix (Takara, Japan) on Roche Light Cycler® 480II System (Roche Diagnostics Ltd., Switzerland). Primer Express Software (Applied Biosystems, Shanghai, China) was used to design PKM2 primer pairs of human genes (Table 1). GAPDH was used as the internal control. The PCR procedure was 95°C for 10 min, followed by 40 cycles of 95°C for 15 s, 60°C for 45 s; one cycle of 95°C for 15 s, 60°C for 1 min; one cycle of 95°C for 15 s, 60°C for 15 s. The relative expression levels of different groups were calculated using the $\Delta\Delta C_T$ method by normalizing to the mRNA expression level of GAPDH. All PCR reactions were performed in triplicate.

Western Blot Analysis

The relationship between PKM2 and tumor-regulated genes was explored by Western blot assays. Transfected cells were harvested, washed twice with PBS, lysed in ice-cold radio immunoprecipitation assay buffer (RIPA; Beyotime, Shanghai, China) containing 0.01% protease and phosphatase inhibitor (Sigma-Aldrich, Shanghai, China), and incubated on ice for 30 min. Then cell lysis was obtained and centrifuged at 12,000×*g* at 4°C for 10 min. Proteins in the supernatant were obtained and quantified by BCA Protein Quantitation Kit (PICPI23223; Thermo Fisher Scientific). About 20–30 µg of protein samples in each load was separated by 10% SDS-PAGE gel and then transferred electrophoretically to a polyvinylidene fluoride membrane (Millipore, Shanghai, China). The membrane was blocked with 5% BSA in PBST and incubated with primary antibodies against PKM2 (Ab133490; 1:1,000 dilution; Abcam), caspase 7 (Ab32419; 1:1,000 dilution; Abcam), matrix metalloproteinase 2 (MMP2) (Ab92536; 1:1,000 dilution; Abcam), HIF1 (#3879s; 1:1,000 dilution; Cell Signaling Technology), Bad (Ab175430; 1:500 dilution; Abcam), vascular endothelial growth factor (VEGF) (Ab175430; 1:500 dilution; Abcam), MMP9 (Ab119906; 1:500 dilution; Abcam), and E-cadherin (#14472; 1:1,000 dilution; Cell Signaling Technology), glyceraldehyde 3-phosphate dehydrogenase (GAPDH) (#5174; 1:1500 dilution; Cell Signaling Technology). Blots were incubated for 1 h at 37°C with goat, anti-mouse, or anti-rabbit secondary antibody (Beyotime), and intensities were measured using enhanced chemiluminescence (ECL; Thermo Scientific, Shanghai, China).

Statistical Analysis

All statistical analyses were conducted using the Graphpad Prism 6.0 software. Data were analyzed by *t*-tests. All experiments were performed with values expressed as mean ± SD. A value of $p<0.05$ was considered statistically significant in all statistical comparisons.

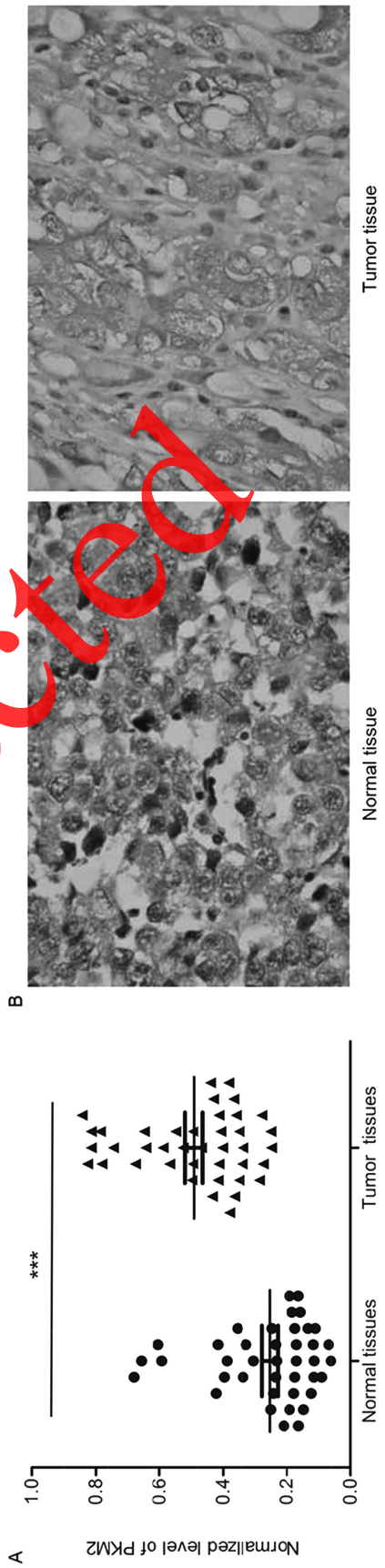

Figure 1. High expression of PKM2 in ovarian tumor tissues. (A) The mRNA levels of PKM2 in tumor tissues were significantly higher than that in normal tissues. $n=40$, mean ± SD. ***$p<0.001$ versus normal tissues. (B) The protein levels of PKM2 in tumor tissues were significantly higher than that in normal tissues.

RESULTS

High Expression of PKM2 in Ovarian Tumor Tissues and Cell Lines

In order to determine the expression levels of PKM2 in normal human ovarian tissue and OC tissue, qRT-PCR and immunohistochemistry assays were performed, and results showed that the mRNA and protein levels of PKM2 in tumor tissues were significantly higher than those in normal tissues ($n=40$, $p<0.001$) (Fig. 1A and B). The mRNA and protein levels of PKM2 in various OC cell lines containing C200, Caov3, SKOV3, HO8910, and OVCAR3 were detected by qRT-PCR and Western blot, respectively. Notably, PKM2 in SKOV3 and OVCAR3 cell lines was expressed much higher than in others ($n=3$, $p<0.01$) (Fig. 2A and B). Because there was a high expression in ovarian tumor tissue and cells, both SKOV3 and OVCAR3 cell lines were selected to carry out our future assays.

Expression of PKM2 in SKOV3 and OVCAR3 Cells After Transfection

In order to detect whether the siRNA-PKM2 or control-siRNA (NC) was transfected successfully, qRT-PCR and Western blot assays were performed. As shown in Figure 3A and B, in the siRNA-PKM2 group, relative mRNA expression levels of PKM2 in both cell lines were notably decreased. Similarly, the protein levels of PKM2 in the siRNA-PKM2 group were also down-regulated. The above results suggest that expression of PKM2 was interfered successfully.

siRNA-PKM2 Inhibits Cell Viability

Cell growth (OD_{450nm}) and proliferation rates were measured by CCK-8. Results showed that after transfection with siRNA-PKM2 or control-siRNA (NC) for 24, 48, and 72 h, cell viability of both SKOV3 and OVCAR3 was markedly weakened in the siRNA-PKM2 group cells in a time-dependent manner ($n=3$, $p<0.01$) (Fig. 4A and B). This suggests that siRNA-PKM2 inhibited cell viability and proliferation.

siRNA-PKM2 Affects Cell Cycle Control

In order to determine whether the inhibitory effect of siRNA-PKM2 on ovarian tumor cell proliferation was mediated by cell cycle, flow cytometry was used. The results revealed that, compared with the control group,

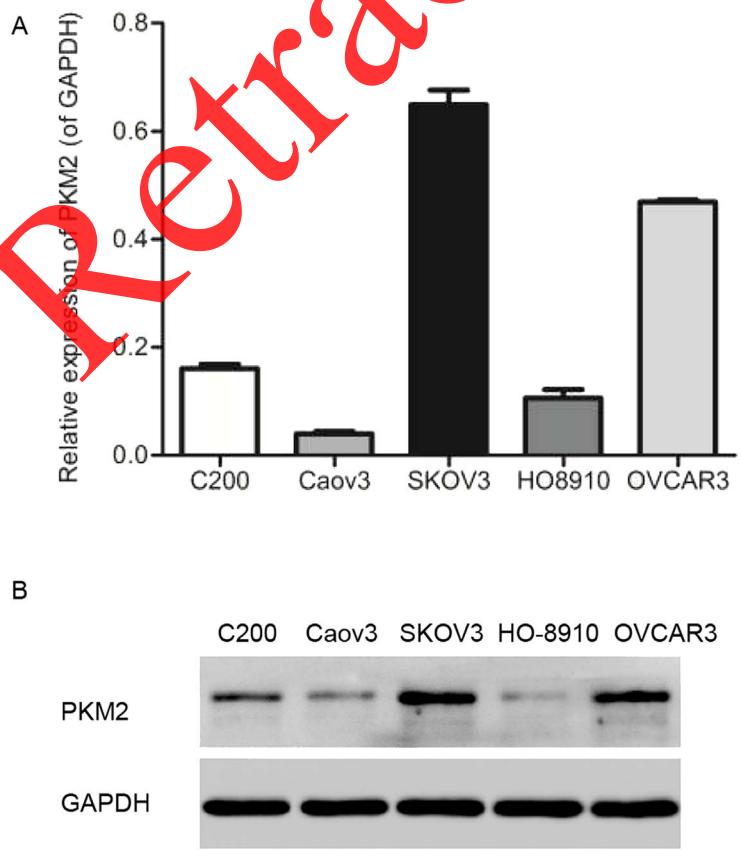

Figure 2. Higher expression of PKM2 in SHOV3 and OVCAR3 cell lines. (A) mRNA expression levels of PKM2 in C200, Caov3, SKOV3, HO8910, and OVCAR3 cell lines. (B) Protein levels of PKM2 in the above ovarian tumor cell lines. $n=3$.

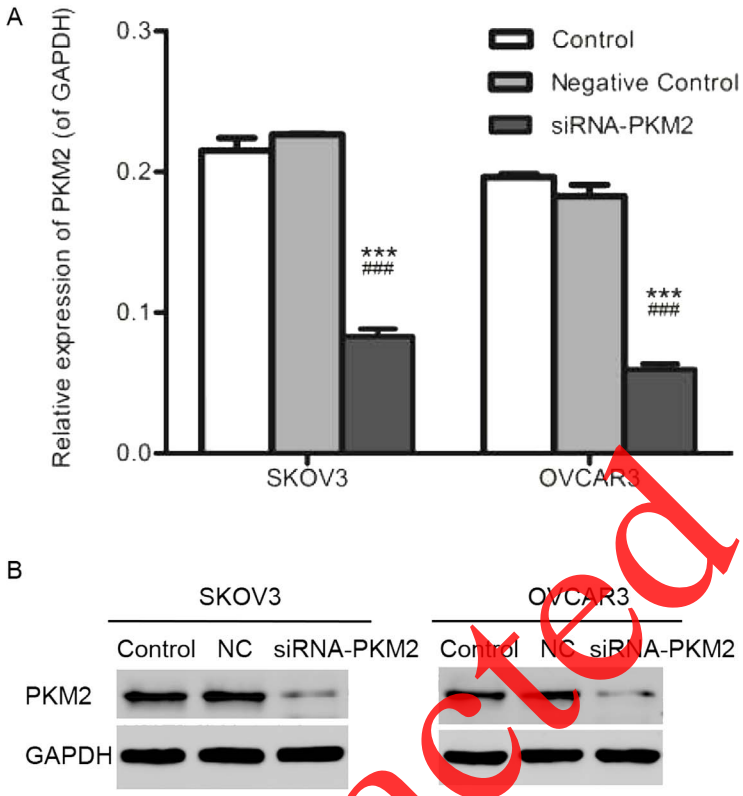

Figure 3. Expression of PKM2 in SKOV3 and OVCAR3 cells after transfection. (A) mRNA expression levels of PKM2 in both SKOV3 and OVCAR3 cells were decreased notably in the siRNA-PKM2 group. (B) The proteins levels of PKM2 in the siRNA-PKM2 group were also downregulated not only in SKOV3 cells but also in OVCAR3 cells. $n=3$, mean ± SD. ***$p<0.001$ versus Control, ###$p<0.001$ versus Negative Control.

the SKOV3 cells in the treatment group were significantly increased in the G_0/G_1 phase ($n=3$, $p<0.01$) (Fig. 5A and B), as well as the OVCAR3 cells ($n=3$, $p<0.01$) (Fig. 5C and D). siRNA-PKM2 induced cell cycle arrest at the G_0/G_1 phase, suggesting that PKM2 might regulate cell proliferation by controlling the G_0/G_1 checkpoint and inducing a specific block in cell cycle progression.

siRNA-PKM2 Induces Cellular Apoptosis

To substantiate cell apoptosis induced by siRNA-PKM2 treatment under various times, Annexin-V/FITC-PI double staining and flow cytometry analysis were performed. The number of apoptotic cells is shown in the lower right quadrant, and the lower left quadrant shows live cells (Fig. 6A and B). The number of apoptotic cells in the siRNA-PKM2 treatment groups was significantly increased compared with the control groups ($n=3$, $p<0.01$) (Fig. 6C). The results suggest that siRNA-PKM2 induced ovarian tumor cell apoptosis.

siRNA-PKM2 Inhibited Cellular Migration and Invasion

Transwell test was performed to explore the effects of siRNA-PKM2 on SKOV3 and OVCAR3 cells. As shown in Figure 7A, treatment with siRNA-PKM2 obviously suppressed the migration and invasion abilities of cells compared with the NC and control groups. The numbers of cells that migrated in the control, NC, and siRNA-PKM2 groups were 112 ± 7, 107 ± 9, and 52 ± 5, respectively, in SKOV3 cells and 136 ± 7, 134 ± 9, and 60 ± 6, respectively, in OVCAR3 cells. The numbers of cells that invaded in the control, NC, and siRNA-PKM2 groups were 77 ± 8, 70 ± 3, and 27 ± 5, respectively, in SKOV3 cells and 88 ± 5, 74 ± 8, and 24 ± 3, respectively, in OVCAR3 cells (Fig. 7B). The results indicate that siRNA-PKM2 inhibited migration and invasion of ovarian tumor cells.

siRNA-PKM2 Regulated the Tumor Suppressor Genes and Oncogenes

In order to further understand the mechanism through which ovarian tumor cell proliferation and metastasis were inhibited by siRNA-PKM2, the mRNA expression levels and protein levels of several tumor-related genes in SKOV3 and OVCAR3 cells were detected by qRT-PCR and Western blot, respectively. As revealed in Figure 8A and C, not only in SKOV3 cells but also in OVCAR3 cells, the mRNA expression levels of the tumor-related

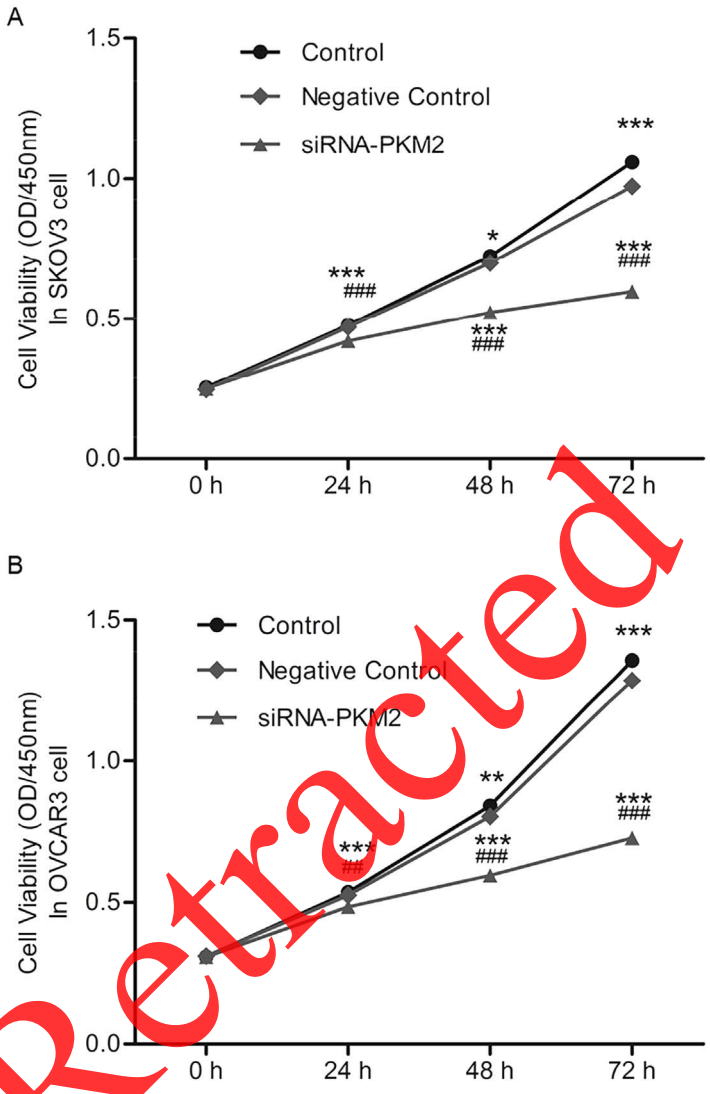

Figure 4. siRNA-PKM2 inhibited cell viability. (A) Cell viability of SKOV3 was weakened markedly in siRNA-PKM2 group cells in a time-dependent manner. (B) Cell viability of OVCAR3 was weakened markedly in siRNA-PKM2 group cells. $n=3$, mean ± SD. $^{**}p<0.01$, $^{***}p<0.001$ versus Control, $\#\#p<0.01$, $\#\#\#p<0.001$ versus Negative Control.

genes caspase 7, Bad, and E-cadherin were upregulated, while MMP2, HIF1a, VEGF, and MMP9 were depressed in the siRNA-PKM2 group compared with the controls. Similarly, the results of protein levels corresponded with the mRNA levels (Fig. 8B and D).

DISCUSSION

OC varies widely in frequency among different geographic regions and ethnic groups, with a high incidence in Northern Europe and the US, and a low incidence in Japan. The majority of cases are sporadic, and only 5% to 10% of OCs are familial. The etiology of OC is poorly understood (15).

The expression of PKM2 in various kinds of cancers has been explored in both in vivo and in vitro studies, while in the aspect of OC, it is nearly unknown. Research on the effects of PKM2 on cell proliferation is always increasing. For instance, it is reported that PKM2 expression was increased and facilitates lactate production in cancer cells (16). Modulation of PKM2 catalytic activity also regulates the synthesis of DNA and lipids that are required for cell proliferation and of NADPH that is required for redox homeostasis (17). In addition to its role as a PK, PKM2 also functions as a protein kinase and as a transcriptional coactivator. These biochemical activities are controlled by allosteric regulators and posttranslational modifications of PKM2 that include acetylation, oxidation, phosphorylation, prolyl hydroxylation, and sumoylation (18). Given its pleiotropic effects on cancer biology, PKM2 represents an attractive target for cancer

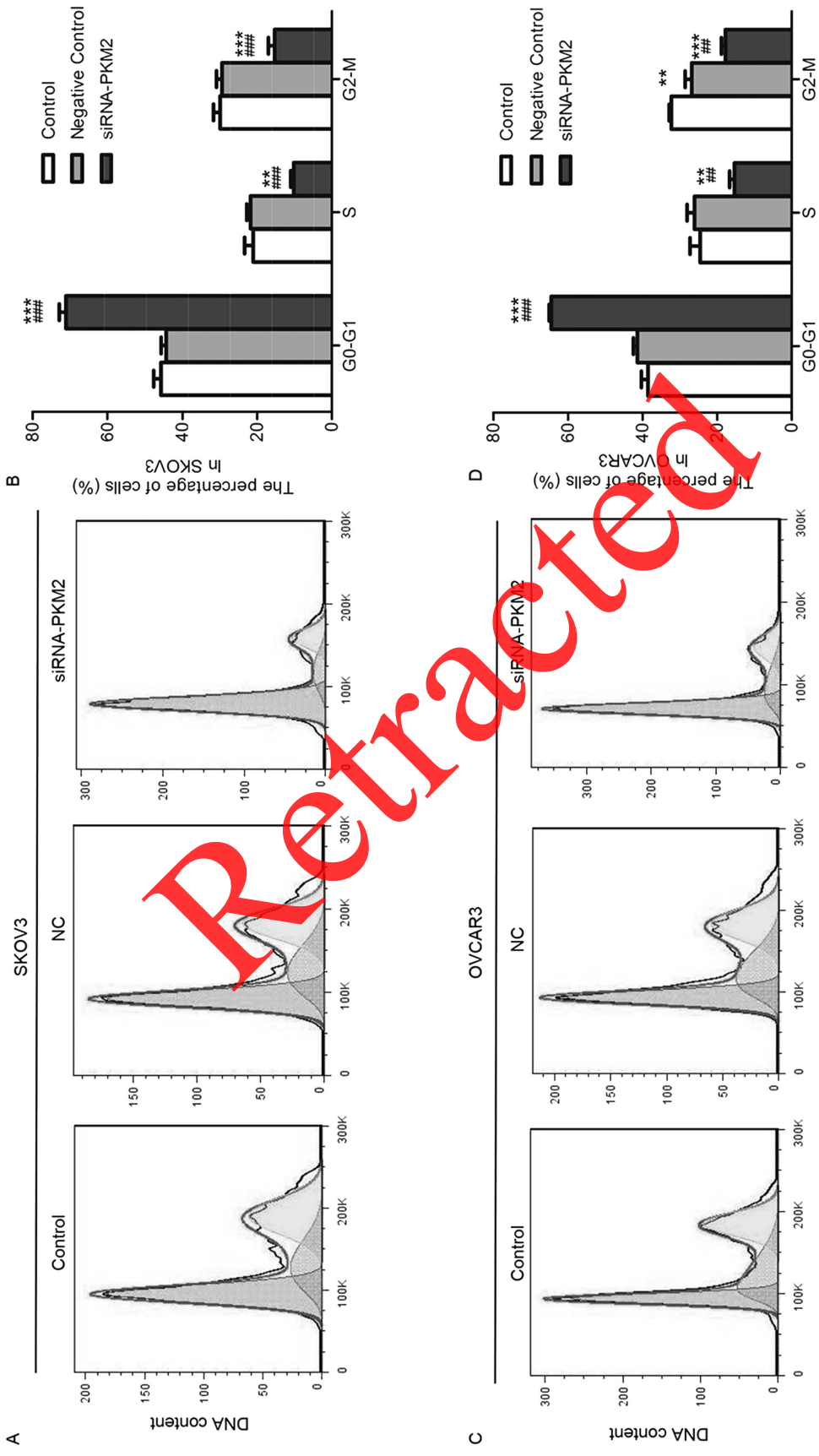

Figure 5. siRNA-PKM2 arrested cell cycle at the G_0/G_1 phase. (A and B) The percentage of G_0/G_1 phase cells of SKOV3 was increased, while the percentages of S and G_2/M phase cells were decreased in the siRNA-PKM2 treatment group. (C, D) The percentage of G_0/G_1 phase cells of OVCAR3 was increased, while the percentage of S and G_2/M phase cells was decreased in the siRNA-PKM2 treatment group. $n = 3$, mean ± SD. $^{**}p < 0.01$, $^{***}p < 0.001$ versus Control; $^{\#\#}p < 0.01$, $^{\#\#\#}p < 0.001$ versus Negative Control.

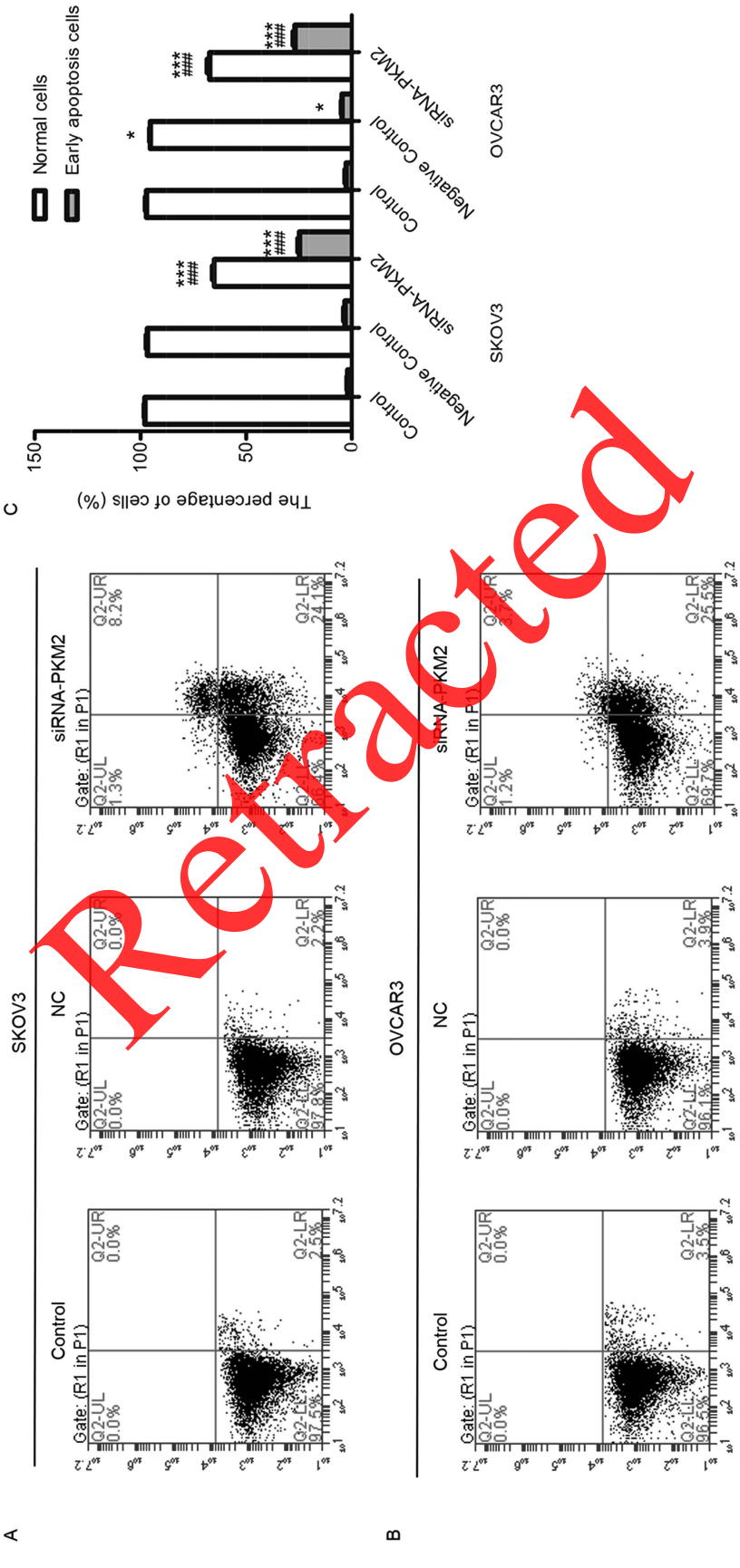

Figure 6. siRNA-PKM2 induced cell apoptosis. (A and B) siRNA-PKM2 induced cell apoptosis of SKOV3 and OVCAR3 cells. (C) siRNA-PKM2 obviously increased the apoptotic population of the two cell lines. $n = 3$, mean ± SD. ***$p < 0.001$ versus Control, ###$p < 0.001$ versus Negative Control.

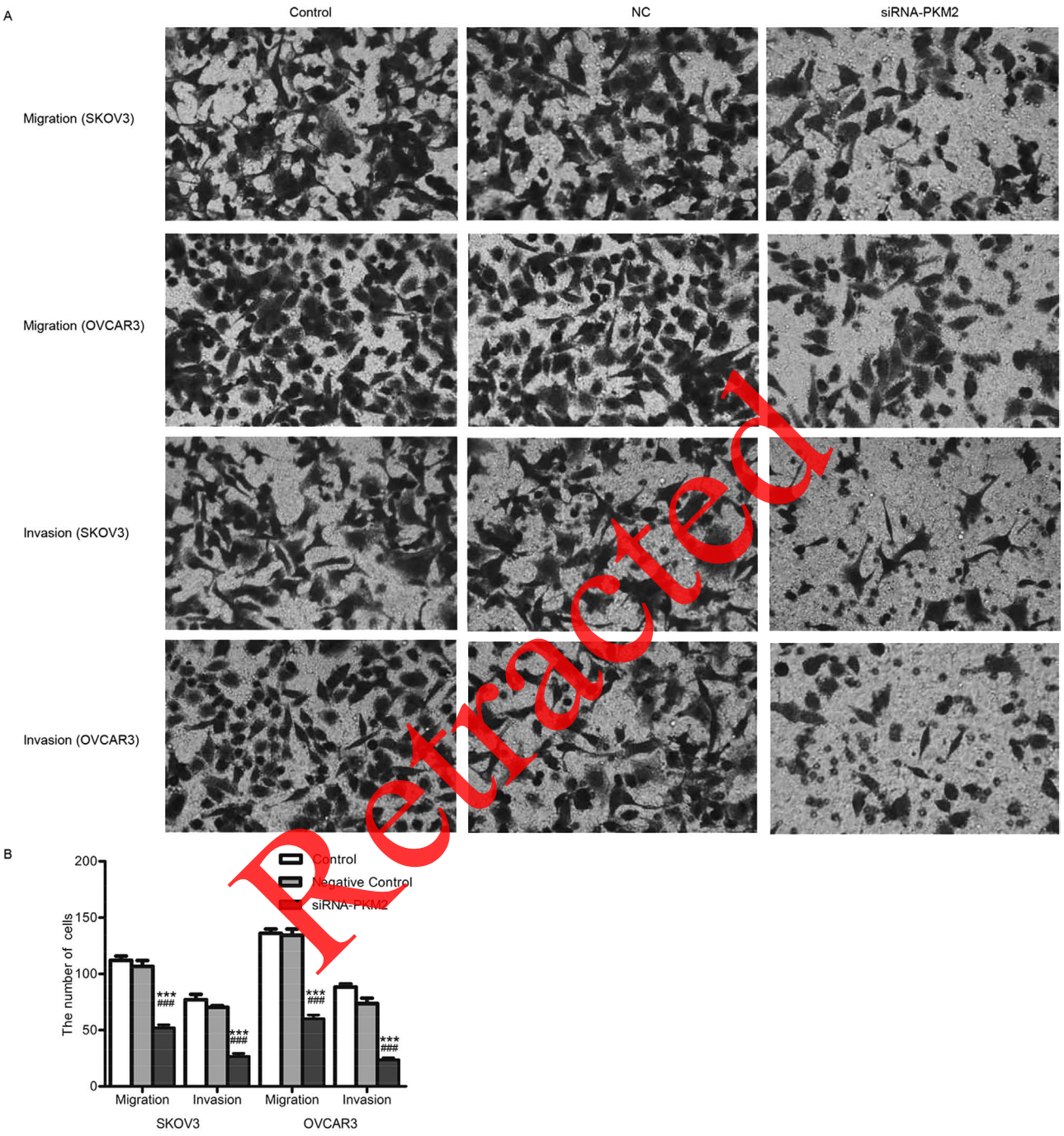

Figure 7. siRNA-PKM2 inhibited migration and invasion of SKOV3 and OVCAR3 cells. (A) The migration and invasion abilities of SKOV3 and OVCAR3 were obviously suppressed by siRNA-PKM2, respectively. (B) The migration and invasion cell numbers of both SKOV3 and OVCAR3 were decreased, respectively. $n = 3$, mean ± SD. ***$p < 0.001$ versus Control, ###$p < 0.001$ versus Negative Control.

therapy (19). Considered together, PKM2 expression was upregulated in various cancer cells and involved in regulating cell proliferation. Likewise, in our present study, knockdown of PKM2 with siRNA inhibited the proliferation of OC cell lines.

This distinct metabolic phenotype, termed as aerobic glycolysis, serves as a metabolic advantage as it provides dividing cells both energy and glycolytic intermediates (phosphor metabolites) that are required as precursors for the synthesis of nucleic acids, amino acids, and lipids

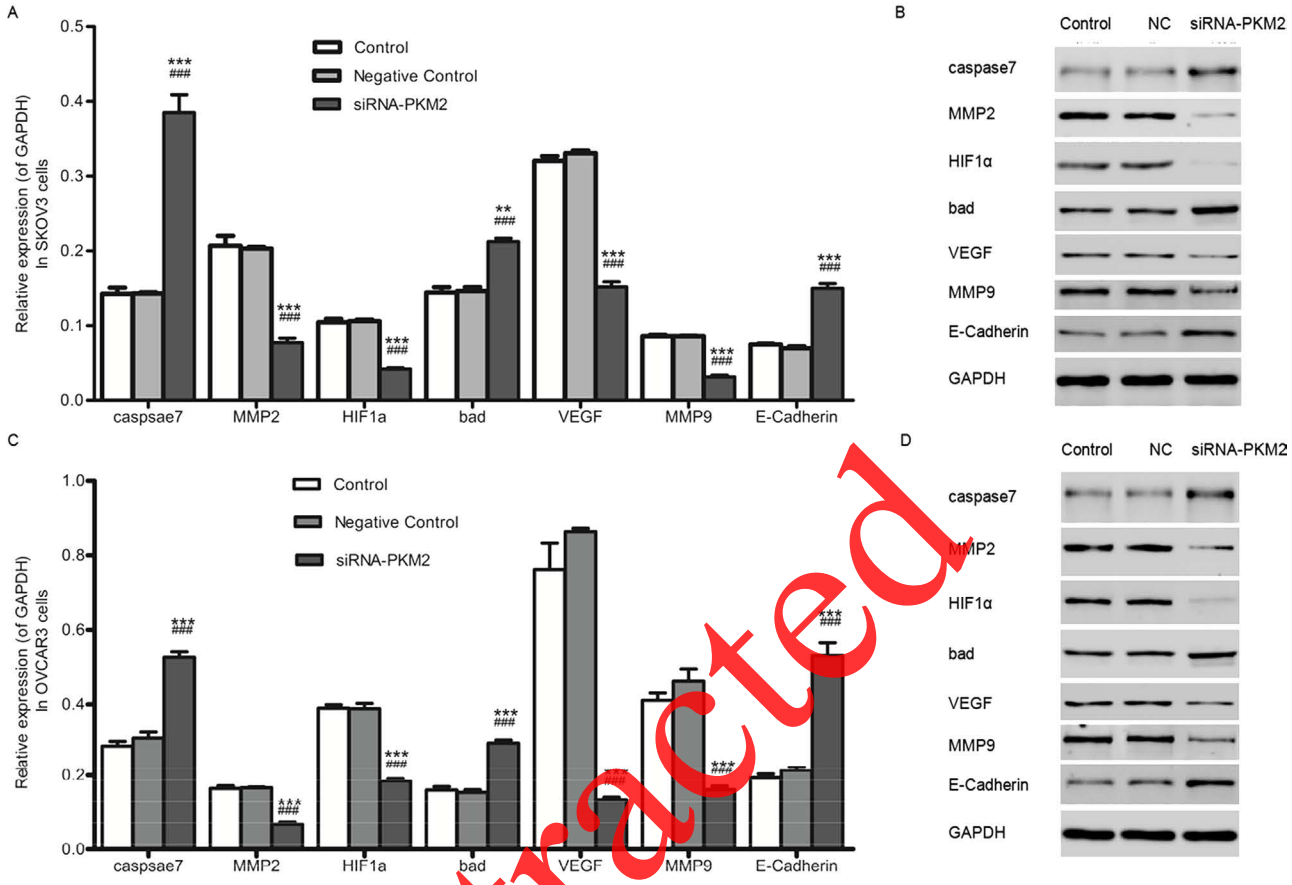

Figure 8. siRNA-PKM2 regulated the tumor suppressor genes and oncogenes. (A and C) The mRNA expression levels of the tumor-related genes caspase 7, Bad, and E-cadherin were upregulated, whereas MMP2, HIF1α, VEGF, and MMP9 were depressed in the siRNA-PKM2 group compared with the controls. (B and D) The protein levels of the tumor-related genes caspase 7, Bad, and E-cadherin were upregulated, whereas MMP2, HIF1α, VEGF, and MMP9 were downregulated. $n=3$, mean±SD. ***$p<0.001$ versus Control, ###$p<0.001$ versus Negative Control.

(20–22). Acidification of the extracellular microenvironment due to increased lactate production may facilitate tumor cell invasion and metastasis (22,23). It has even been proposed that aerobic glycolysis is an early and essentially irreversible step that leads to tumorigenesis (24). Recent results show that upregulation of glycolytic enzymes plays a crucial role in cancer. Among these enzymes, PKM2 comprises one of the most unregulated genes in cancers (25–27). It is shown that expression of PKM2 in cancer cells is essential for the establishment of aerobic glycolysis and provides a selective growth advantage for tumor cells in vivo (27). A high level of this glycolytic intermediate reflects sufficient amounts of phosphor-metabolites and induces reassociation of the dimeric form of PKM2 to the highly active tetrameric form, thus shifting tumor metabolism from the synthesis of cell building blocks to energy regeneration (4,28). So it is believed that PKM2 plays a key role in the channeling of glucose carbons into either catabolic or anabolic pathways (29,30). Taken together, PKM2 has a function in cancer cell metastasis, and existing reports agree with our current study that transfection of cells with siRNA-PKM2 caused the inhibition of cell metastasis.

PKM2 may play a critical role in pathways leading to cell proliferation and metastasis, while the precise mechanism is still unknown. In order to explore this, we proved that siRNA-PKM2 affects the expression of several tumor-related genes. Knockdown of PKM2 with siRNA resulted in the upregulation of tumor suppressor gene caspase 7, Bad, and E-cadherin, while oncogenes, containing MMP2, HIF1α, VEGF, and MMP9, were downregulated. Among them, MMP2 and MMP9 are MMP members (31). Human prostate cancer cell invasion is inhibited by finasteride through MMP2 and MMP9 downregulation (32). It is also reported that MMP2 may play a role in the migration of tumor cells (33). E-cadherin, together with Snai1 and Twist, plays a vital role in the EMT (epithelial–mesenchymal transition) process, which is closely associated with tumor cell

metastasis (34). The genes identified in this SVM classifier are in commonly deregulated pathways in OC (35–37). BRCA1/BRCA2, p53, and the EMT phenotype (particularly E-cadherin expression) have independently been reported to be prognostic factors for chemotherapy resistance and survival of women with ovarian carcinoma. Taken together, it was very likely that the inhibition of cell proliferation and metastasis in OC cell line by knockdown of PKM2 may be through these tumor-related genes. Further studies are necessary to determine the functional role of PKM2 in cancer.

CONCLUSION

In conclusion, siRNA-PKM2 was expressed much higher in OC tissues and cell lines. Here we first proved that siRNA-PKM2 inhibited proliferation and metastasis of SKOV3 and OVCAR3 OC cell lines. We also found that several tumor suppressor genes and oncogenes were up- and downregulated. Our work contributed to discovering the functional role of PKM2 in cancer.

REFERENCES

1. Slamon, D. J.; Godolphin, W.; Jones, L. A.; Holt, J. A.; Wong, S. G.; Keith, D. E.; Levin, W. J.; Stuart, S. G.; Udove, J.; Ullrich, A. Studies of the HER-2/neu proto-oncogene in human breast and ovarian cancer. Science 244:707–712; 1989.
2. Holschneider, C. H.; Berek, J. S. Ovarian cancer: Epidemiology, biology, and prognostic factors. Semin. Surg. Oncol. 19(1):3–10; 2000.
3. Bast, Jr. R. C.; Urban, N.; Shridhar, V.; Smith, D.; Zhang, Z.; Skates, S.; Lu, K.; Liu, J.; Fishman, D.; Mills, G. Early detection of ovarian cancer: Promise and reality. In M. S. Stack, D. A. Fishman, eds. Ovarian cancer. New York: Springer; 2002:61–97.
4. Mazurek, S. Pyruvate kinase type M2: A key regulator of the metabolic budget system in tumor cells. Int. J. Biochem. Cell Biol. 43:969–980; 2011.
5. Schneider, J.; Morr, H.; Velcovsky, H.; Weisse, G.; Eigenbrodt, E. Quantitative detection of tumor M2-pyruvate kinase in plasma of patients with lung cancer in comparison to other lung diseases. Cancer Detect. Prev. 24:531–535; 1999.
6. Yuan, Y.; Guo-Qing, P.; Yan, T.; Hong-Lin, Y.; Gong-Hua, H.; Cai-Gao, Z. A study of PKM2, PFK-1, and ANT1 expressions in cervical biopsy tissues in China. Med. Oncol. 29:2904–2910; 2012.
7. Zhou, C. F.; Li, X. B.; Sun, H.; Zhang, B.; Han, Y. S.; Jiang, Y.; Zhuang, Q. L.; Fang, J.; Wu, G. H. Pyruvate kinase type M2 is upregulated in colorectal cancer and promotes proliferation and migration of colon cancer cells. IUBMB Life 64:775–782; 2012.
8. Ma, Y.; Peng, J.; Liu, W.; Zhang, P.; Huang, L.; Gao, B.; Shen, T.; Zhou, Y.; Chen, H.; Chu, Z. Proteomics identification of desmin as a potential oncofetal diagnostic and prognostic biomarker in colorectal cancer. Mol. Cell. Proteomics 8:1878–1890; 2009.
9. Gao, X.; Wang, H.; Yang, J. J.; Liu, X.; Liu, Z.-R. Pyruvate kinase M2 regulates gene transcription by acting as a protein kinase. Mol. Cell 45:598–609; 2012.
10. Shi, H. S.; Li, D.; Zhang, J.; Wang, Y. S.; Yang, L.; Zhang, H. l.; Wang, X. H.; Mu, B.; Wang, W.; Ma, Y. Silencing of pkm2 increases the efficacy of docetaxel in human lung cancer xenografts in mice. Cancer Sci. 101: 1447–1453; 2010.
11. Martinez-Balibrea, E.; Plasencia, C.; Ginés, A.; Martinez-Cardús, A.; Musulén, E.; Aguilera, R.; Manzano, J. L.; Neamati, N.; Abad, A. A proteomic approach links decreased pyruvate kinase M2 expression to oxaliplatin resistance in patients with colorectal cancer and in human cell lines. Mol. Cancer Ther. 8:771–778; 2009.
12. Peng, X.-C.; Gong, F.-M.; Zhao, Y.-W.; Zhou, L.-X.; Xie, Y.-W.; Liao, H.-L.; Lin, H.-J.; Li, Z.-Y.; Tang, M.-H.; Tong, A.-P. Comparative proteomic approach identifies PKM2 and cofilin-1 as potential diagnostic, prognostic and therapeutic targets for pulmonary adenocarcinoma. PLoS One 6:e27309; 2011.
13. Marshall, M.; Goldberg, D.; Neal, F.; Millar, D. Enzymes of glucose metabolism in carcinoma of the cervix and endometrium of the human uterus. Br. J. Cancer 37:990; 1978.
14. Kaura, B.; Bagga, R.; Patel, F. D. Evaluation of the pyruvate kinase isoenzyme tumor (Tu M2-PK) as a tumor marker for cervical carcinoma. J. Obstet. Gynaecol. Res. 30:193–196; 2004.
15. Casagrande, J.; Pike, M.; Ross, R.; Louie, E.; Roy, S.; Henderson, B. "Incessant ovulation" and ovarian cancer. Lancet 314:170–173; 1979.
16. Chaneton, B.; Gottlieb, E. Rocking cell metabolism: Revised functions of the key glycolytic regulator PKM2 in cancer. Trends Biochem. Sci. 37:309–316; 2012.
17. Israelsen, W. J.; Dayton, T. L.; Davidson, S. M.; Fiske, B. P.; Hosios, A. M.; Bellinger, G.; Li, J.; Yu, Y.; Sasaki, M.; Horner, J. W. PKM2 isoform-specific deletion reveals a differential requirement for pyruvate kinase in tumor cells. Cell 155:397–409; 2013.
18. Wong, N.; De Melo, J.; Tang, D. PKM2, a central point of regulation in cancer metabolism. Int. J. Cell Biol. 2013:242513; 2013.
19. Jiang, Y.; Li, X.; Yang, W.; Hawke, D. H.; Zheng, Y.; Xia, Y.; Aldape, K.; Wei, C.; Guo, F.; Chen, Y. PKM2 regulates chromosome segregation and mitosis progression of tumor cells. Mol. Cell 53:75–87; 2014.
20. Ortega, Á. D.; Sánchez-Aragó, M.; Giner-Sánchez, D.; Sánchez-Cenizo, L.; Willers, I.; Cuezva, J. M. Glucose avidity of carcinomas. Cancer Lett. 276:125–135; 2009.
21. Gupta, V.; Bamezai, R. N. Human pyruvate kinase M2: A multifunctional protein. Protein Sci. 19:2031–2044; 2010.
22. Gillies, R. J.; Gatenby, R. A. Adaptive landscapes and emergent phenotypes: Why do cancers have high glycolysis? J. Bioenerg. Biomembr. 39:251–257; 2007.
23. Goetze, K.; Walenta, S.; Ksiazkiewicz, M.; Kunz-Schughart, L. A.; Mueller-Klieser, W. Lactate enhances motility of tumor cells and inhibits monocyte migration and cytokine release. Int. J. Oncol. 39:453–463; 2011.
24. Warburg, O.; On the origin of cancer cells. Science 123: 309–314; 1956.
25. Altenberg, B. A.; Greulich, K. Genes of glycolysis are ubiquitously overexpressed in 24 cancer classes. Genomics 84:1014–1020; 2004.
26. Majumder, P. K.; Febbo, P. G.; Bikoff, R.; Berger, R.; Xue, Q.; McMahon, L. M.; Manola, J.; Brugarolas, J.; McDonnell, T. J.; Golub, T. R. mTOR inhibition reverses Akt-dependent prostate intraepithelial neoplasia through

regulation of apoptotic and HIF-1-dependent pathways. Nat. Med. 10:594–601; 2004.
27. Christofk, H. R.; Vander Heiden, M. G.; Harris, M. H.; Ramanathan, A.; Gerszten, R. E.; Wei, R.; Fleming, M. D.; Schreiber, S. L.; Cantley, L. C. The M2 splice isoform of pyruvate kinase is important for cancer metabolism and tumour growth. Nature 452:230–233; 2008.
28. Mazurek, S.; Boschek, C. B.; Hugo, F.; Eigenbrodt, E. Pyruvate kinase type M2 and its role in tumor growth and spreading. Semin. Cancer Biol. 15(4):300–308; 2005.
29. Christofk, H. R.; Vander Heiden, M. G.; Wu, N.; Asara, J. M.; Cantley, L. C. Pyruvate kinase M2 is a phosphotyrosine-binding protein. Nature 452:181–186; 2008.
30. Hitosugi, T.; Kang, S.; Vander Heiden, M. G.; Chung, T.-W.; Elf, S.; Lythgoe, K.; Dong, S.; Lonial, S.; Wang, X.; Chen, G. Z. Tyrosine phosphorylation inhibits PKM2 to promote the Warburg effect and tumor growth. Sci. Signal. 2:ra73; 2009.
31. Chakrabarti, J.; Chatterjee, A.; Mitra, A.; Chattopadhyay, N. Membrane-associated MMP-2 in human cervical cancer. J. Environ. Pathol. Toxicol. Oncol. 22; 2003.
32. Moroz, A.; Delella, F. K.; Almeida, R.; Lacorte, L. M.; Favaro, W. J.; Deffune, E.; Felisbino, S. L. Finasteride inhibits human prostate cancer cell invasion through MMP2 and MMP9 downregulation. PLoS One 30;8(12):e84757; 2013.
33. Ansieau, S.; Courtois-Cox, S.; Morel, A.-P.; Puisieux, A. Failsafe program escape and EMT: A deleterious partnership. Semin. Cancer Biol. 21(6):392–396; 2011.
34. Tiwari, N.; Gheldof, A.; Tatari, M.; Christofori, G. EMT as the ultimate survival mechanism of cancer cells. Semin. Cancer Biol. 22(3):194–207; 2012.
35. Cancer Genome Atlas Research Network. Integrated genomic analyses of ovarian carcinoma. Nature 474:609–615; 2011.
36. Köbel, M.; Reuss, A.; Bois, A. D.; Kommoss, S.; Kommoss, F.; Gao, D.; Kalloger, S. E.; Huntsman, D. G.; Gilks, C. B. The biological and clinical value of p53 expression in pelvic high-grade serous carcinomas. J. Pathol. 222:191–198; 2010.
37. Vencken, P.; Kriege, M.; Hoogwerf, D.; Beugelink, S.; van der Burg, M.; Hooning, M.; Berns, E.; Jager, A.; Collée, M.; Burger, C. Chemosensitivity and outcome of BRCA1- and BRCA2-associated ovarian cancer patients after first-line chemotherapy compared with sporadic ovarian cancer patients. Ann. Oncol. 22(6):1346–1352; 2011.